PHOTOSYNTHETICA
International Journal for Photosynthesis Research

DOI 10.32615/ps.2021.006 PHOTOSYNTHETICA 59 (1): 148-159, 2021

Inhibition of photosynthesis in *Melia azedarach* and *Ligustrum lucidum* induced by manganese toxicity using OJIP chlorophyll *a* fluorescence transient

M.S. LIU[**], X.H. HUANG[**], R.J. WANG[***], H.Y. XU[**], and F. ZHU[*,+]

College of Landscape Architecture and Art Design, Hunan Agricultural University, 410128 Changsha, China[*]
College of Life Science and Technology, Central-South University of Forestry and Technology, 410004 Changsha, China[**]
Guangxi Key Laboratory of Superior Trees Resource Cultivation, Guangxi Zhuang Autonomous 11 Region Forestry Research Institute, Nanning, China[***]

Abstract

Manganese (Mn) excess is a major abiotic stress for plant growth. In the present study, we investigated the effects of Mn on photosynthesis in *Ligustrum lucidum* and *Melia azedarach* leaves using chlorophyll fluorescence transients. Both plant species were exposed to two Mn concentrations (0.5 and 1 mmol) for 10 and 30 d. Results showed that excess Mn significantly inhibited photosynthesis. With the increase of Mn concentration and stress time, the inhibition was more serious. Mn stress impaired PSII at the donor and the acceptor side by damaging the oxygen-evolving complex and limiting electron transport downstream of Q_A in both trees. A significant decline in 820 nm reflection curve absorption was observed in *M. azedarach*, suggesting that the oxidization-reduction reactions in PSI were inhibited but this phenomenon was not observed in *L. lucidum*. Therefore, excess Mn impaired the whole electron transport chain associated with inactive PSII reaction centers in *Ligustrum lucidum* and inhibited oxidization-reduction reactions in PSI in *M. azedarach*.

Keywords: energy conversion efficiency; heavy metal stress; JIP-test; OJIP curve.

Highlights

- Nonstomatal factors reduced CO_2 assimilation of *Ligustrum lucidum* and *Melia azedarach* under Mn excess
- Mn excess caused the damage to PSII oxygen-evolving system in both species
- *Ligustrum lucidum* might be more tolerant to Mn stress than *Melia azedarach*

Received 17 July 2020
Accepted 18 January 2021
Published online 18 February 2021

[+]Corresponding author
e-mail: csuftzf@163.com
phone: 8615873162712
fax: 0731-85623458

Abbreviations: ABS/RC – absorption flux (of antenna Chls) per RC (also a measure of PSII apparent antenna size); CE – carboxylation efficiency; C_i – intercellular CO_2 concentration; DI_0/RC – dissipated energy flux per RC at t = 0; F_0 – minimal fluorescence yield of the dark-adapted state; F_J – fluorescence intensity at the J-step (2 ms); F_K – fluorescence intensity at 300 μs; F_M – maximum fluorescence yield of the dark-adapted state; F_V/F_M – maximum quantum use efficiency; g_s – stomatal conductance; IP-phase – the efficiency of electron transport around the PSI; M_0 – approximated initial slope of the fluorescence transient; MR_0 – first reliable recorded fluorescence at 0.7 ms; MR_{min} – the minimum fluorescence intensity; OEC – oxygen-evolving complex; PI_{ABS} – performance index; P_N – maximum net photosynthetic rate; RE_0/RC – the flux of electrons transferred from Q_A^- to final PSI acceptors per PSII at t = 0; S_m – normalized total complementary area above the OJIP transient (reflecting single-turnover Q_A reduction events); TR_0/RC – trapped energy flux (leading to Q_A reduction) per RC at t = 0; V_{PSI} – maximum decrease in slope in the range of 0.7–3 ms of MR/MR_0; $V_{PSI+PSII}$ – maximum increase in slope in the range of 7–300 ms of MR/MR_0; δ_{R0} – efficiency with which an electron can move from the reduced intersystem electron acceptors to the PSI end electron acceptors; Φ_{E0} – quantum yield for electron transport; ψ_{E0} – probability that a trapped exciton moves an electron into the electron transport chain beyond Q_A.

Acknowledgements: This research was funded by the National Natural Science Foundation of China (32072672), the Key Research and Development Project of Hunan Province (2017NK2171), the Scientific Innovation Fund for Post-graduates of Central South University of Forestry and Technology (20181007), and the Scientific Innovation Fund for Post-graduates of Central South University of Forestry and Technology (CX20192062).

Conflict of interest: The authors declare that they have no conflict of interest.

Introduction

With the extension and enhancement of human activities, such as mining and industrial disposal (He *et al*. 2012), heavy metals have become a worldwide concern. In nature, heavy metals are difficult to degrade in soil, so they can exist in soil for a long time. Plants growing in metal-contaminated areas show several disturbances related to physiological and biochemical processes, such as photosynthesis (Demmig-Adams *et al*. 2017). Photosynthesis is a process by which plants convert light energy into chemical energy to produce sugars and other organic compounds (Qiao *et al*. 2012). Plants affected by heavy metals have shown inhibition of stomatal conductance (g_s), photosynthetic rate (P_N), carboxylation efficiency (CE), and activity of PSI and PSII, leading to reduced plant growth and biomass.

The disruptive effect of heavy metals on plant photosynthesis is a common phenomenon observed in a wide range of plants (Li *et al.* 2010, Moradi and Ehsanzadeh 2015). Many studies (Miyata *et al*. 2015, Huang *et al*. 2018) have shown that PSII, as the first protein complex in light-dependent reactions, is very sensitive to heavy metal stress. The damage caused by heavy metals to PSII includes that on the donor side (Dewez *et al*. 2005), the acceptor side (Barón *et al*. 1995), and the reaction centers (Fodor 2002). Previous studies have found that copper stress damages the oxygen-evolving complex (OEC) (Rijstenbil *et al*. 1994) and the electron transport of PSII (Yruela *et al*. 1996), resulting in a reduction in the quantum efficiency of PSII. The positive O-step, J-step, L-band, and K-band in chlorophyll (Chl) *a* fluorescence transients were observed in Mn-treated *Citrus grandis* seedlings, suggesting that Mn impairs PSII behavior (Li *et al*. 2010). Gururani *et al*. (2013) have reported that the positive K-bands and L-bands appear under heavy metal stress. Che *et al*. (2018) observed that under stress from excess copper, the Chl fluorescence transient curves change from OJIP to OKJIP. The positive K-band and the reduction of proteins of the OEC suggest that excess copper damages the OEC at the donor side of PSII and affects the activity of PSII. Liang *et al*. (2019) have reported that excess Mn inhibits PSII electron transport from the donor side to the acceptor side, which may be caused by the damaged OEC in *L. lucidum*. It has been also reported that damage caused by Cd toxicity on electron transport occurs on both the donor and acceptor sides of PSII (Sigfridsson *et al*. 2004). Farmer and Mueller (2013) found that heavy metals inhibit PSII and increase the production of $^1O_2$. At the same time, the stress also causes the photoinhibition of the PSII (Aranjuelo *et al*. 2014, Yang *et al*. 2020). When the absorption of light is more than light requirments for photosythesis, singlet oxygen is produced in PSII which can cause photoinhibition of PSII. Pätsikkä *et al.* (1998) found that excess copper caused photoinhibiton of PSII for the electron transport from the donor side to P_{680}^+. It is generally recognized that in most plants, environmental stress usually causes selective photodamage of PSII, while plants can protect PSI under environmental stress (Kono *et al*. 2014). The study has found that under stressful conditions, when the electron flow from PSII to PSI exceeds the capacity of PSI electron acceptors, the acceptor side becomes overreduced. As a result, PSI is also vulnerable to damage (Suorsa *et al*. 2012, Tikkanen *et al*. 2014, Zhang *et al*. 2016). Millaleo *et al*. (2013) have found that PSI is the main target of Mn toxicity in *Arabidopsis* plants. They have also found that under the Mn excess, the state of P700 photooxidation (P_{700}^+) significantly decreases as compared to controls.

The decrease in CE response to environmental stress may be caused by the impaired electron transport chain. González and Lynch (2006) have reported a reduction of leaf CE, which can be attributed to the significant decline of total Chl contents, rather than changes in stomatal conductance and transpiration rates. Chu *et al*. (2018) have found that in *Schima superba* plant, the electron transport of PSII acceptor and donor sides is blocked, and the reduction of CE is attributed to the inactivity of the photosynthesis rather than the stomatal limitation for the decrease in g_s but the increase in intercellular CO_2 concentration (C_i). In contrast, the drought stress decreased P_N significantly for the great decline in stomatal conductance in both sun and shade plants (Valladares and Pearcy 2002). Suresh *et al*. (1987) have observed that excess Mn decreases stomatal conductance and transpiration rate, indicating that Mn is involved in stomatal regulation. Under drought stress, stomatal limitation leads to the reduction of CO_2 uptake, C_i, and CE of leaves (Flexas and Medrano 2002). The toxicity of heavy metals in plants depends on the type of heavy metal, the species of plant, and the concentration of heavy metals (Nagajyoti *et al*. 2010).

Mn is an essential trace element for plant metabolism and photosynthesis (Kitao *et al*. 1997, Li *et al.* 2010). However, excess Mn can decrease yield production and quality in crops (Xue *et al*. 2015). Mn excess is a major abiotic stress in plant agriculture worldwide (Xue *et al*. 2015). *Melia azedarach* (*M. azedarach*) is a preferred tree species for afforestation in industrial and mining areas, and it is also one of the tree species used for artificial afforestation in abandoned coal-skilled stone fields (Khattak and Jabeen 2012). *Ligustrum lucidum* (*L. lucidum*) has been verified to be an excellent tree species for remediation of soil ecosystems polluted by heavy metals (Tong *et al*. 2011). For phytoremediation, the native plants may be a better choice because they are better adapted to local climate conditions (Trikshiqi and Rexha 2015). *M. azedarach* and *L. lucidum* are common native tree species in Southern China, which are widely used in afforestation. Previous study has found that they have high tolerance in Cd-, Hg- or As-contaminated soils, showing great potential in phytoremediation of heavy metal-contaminated environments (Tong *et al.* 2011, Su *et al*. 2017). In this study, we investigated the effects of Mn stress on the photosynthetic activity and CE of *M. azedarach* and *L. lucidum.* Besides, the different states of photosynthetic system of *M. azedarach* and *L. lucidum* under excess Mn stress were also discussed. Collectively,

our findings provided a theoretical basis for the selection of resistant tree species for the phytoremediation of Mn-polluted environments.

Materials and methods

Growth conditions and experimental design: This study was carried out in a greenhouse at Central South University of Forestry and Technology (CSUFT), Changsha City, Hunan Province of China (28°8'12"N, 112°59'36"E). The plants were cultured at temperatures of 30/25°C and under a 12/12-h day/night cycle and maximum PAR of about 1,400 μmol(photon) m^{-2} s^{-1}. Non-heavy metal-contaminated soil samples were collected at a depth of 5–20 cm from a garden at the CSUFT campus. Soil samples were sieved through 5 × 5 mm sieves to remove large debris and rocks and then air-dried at room temperature. The chemical composition of the soil samples was as follows: pH 5.5, 0.36 g(N) kg^{-1}, 12.18 g(C) kg^{-1}, and 463.53 mg(Mn) kg^{-1}.

In the present study, 2-year-old *L. lucidum* plants (average diameter of 9.0 mm and average plant height of 133.0 cm) and 2-year-old *M. azedarach* plants (average diameter of 5.4 mm and average tree height of 73.3 cm) were purchased from a local nursery. The plants were individually transplanted into plastic pots (diameter of 25.4 cm and height of 17.8 cm) with one plant per pot, and each plot was filled with 5 kg of air-dried soil. After transplantation, the pots were maintained in the greenhouse for four months before Mn treatment. About 400 mL of pure water was added into each pot every 2 d.

Three treatments with different Mn contents were set up in this study as follows: (*1*) soil sample + Mn solutions until the soil contained 4,365 mg of Mn per pot (designated as L1), (*2*) soil sample + Mn solutions until the soil contained 8,730 mg of Mn per pot (designated as L2), and (*3*) soil sample + distilled water (designated as the control). For the Mn-treated soil, distilled water containing 0.5 mmol and 1 mmol from $MnCl_2 \cdot 5H_2O$ was added to the pots every other day at a rate of 400 mL per day for 20 d. For the control (CK), about 400 mL of distilled water without Mn was added into the pots. Each Mn treatment was replicated five times. Thirty pots were set in this experiment including 15 pots (5 pots for CK, 5 pots for L1, and 5 pots for L2) for *L. lucidum* and 15 pots (5 pots for CK, 5 pots for L1, and 5 pots for L2) for *M. azedarach*. Each pot contained one plant. All measurements were conducted on three fully expanded and similar-sized leaves from each *L. lucidum* and *M. azedarach* plant and a mean value was then obtained.

Gas exchange: P_N, CE, g_s, and C_i were determined by *LI-COR 6400* portable photosynthesis system (*LI-COR Bioscience*, Lincoln, NE, USA). Under the conditions of greenhouse temperature (30°C) and light intensity [1,400 μmol(photon) m^{-2} s^{-1}], concentrations of ambient CO_2 (400, 350, 300, 250, 200, 150, 100, 50 ppm) were set to determine P_N and C_i of the same leaf, and the response curve of P_N–C_i was drawn. The initial slope of the curve was CE, $CE = P_N/C_i$.

Chl fluorescence parameters (FPs) and JIP-test: Fast Chl *a* fluorescence was determined by *M-PEA* (*Multi-functional Plant Efficiency Analyzer*, *Hansatech Instrument*, UK). The OJIP transient was induced by the red light of about 5,000 μmol(photon) m^{-2} s^{-1}, provided by an array of three light-emitting diodes (peak 650 nm), recorded at 128 points and measured daily at 8:30–11:00 h. All measurements were conducted with dark-adapted plants at room temperature. The OJIP transient was analyzed by the JIP-test (Stirbet *et al*. 2018), which defines the flux ratios [Φ_{E0} (= ET_0/ABS), ψ_{E0} (= 1 – V_J), δ_{R0} (= RE_0/ET_0)], performance indexes [PI_{ABS} = (RC/ABS × [$\varphi_{P0}/(1 - \varphi_{P0})$] × [$\psi_{E0}/(1 - \psi_{E0})$])], the maximum quantum use efficiency [F_V/F_M (= $(F_M - F_0)/F_M$)], normalized total complementary area above the OJIP transient (reflecting single-turnover Q_A reduction events) [S_m (= Area/F_V)], approximated initial slope of the fluorescence transient [M_0 = (4[$F_{300\ \mu s} - F_0$]/[$F_M - F_0$])], and the specific energy fluxes (per active PSII) [ABS/RC (= [M_0/V_J]/φ_{P0}), TR_0/RC (= M_0/V_J), RE_0/RC (= [M_0/V_J] × ψ_{R0}), and DI_0/RC (= ABS/RC – TR_0/RC)].

W_{OK} indicated the relative fluorescence between O and K, while ΔW_{OK} indicated the difference between the CK groups and the treated groups:

$$W_{OK} = (F_t - F_0)/(F_K - F_0)$$

$$\Delta W_{OK} = W_{OK} - W_{OK(control)}$$

V_t indicated the relative fluorescence between O and P, while ΔV_t indicated the difference between the CK groups and the treated groups:

$$V_t = (F_t - F_0)/(F_M - F_0)$$

$$\Delta V_t = V_t - V_{t(control)}$$

IP-phase indicates the amplitude of the IP-phase or the last and slowest rate-limiting step of the photosynthetic electron transport chain (Ceppi *et al*. 2012).

$$\text{IP-phase} = (F_t - F_I)/(F_I - F_0)$$

F_0 is the minimal recorded fluorescence intensity, F_K and F_I are the fluorescence intensities at K-step (300 μs) and I-step (30 ms) of OJIP, respectively, and F_M is the maximal recorded fluorescence intensity, at the peak P of OJIP.

The kinetics of prompt fluorescence and modulated 820-nm reflection: The red-light absorbance at a wavelength of 820 nm was measured by the *Multifunctional Plant Efficiency Analyzer* (*M-PEA*, *Hansatech*, Norfolk, UK). The 820-nm red light absorbance was induced by a red-light pulse of about 5,000 μmol(photon) m^{-2} s^{-1}, recorded at 128 points, and measured daily at 8:30–11:00 h. Before measuring, the leaves were dark-adapted at room temperature for 40 min.

The oxidation of P700 and plastocyanin (PC) can increase the absorbance in the 800–850 nm range. After dark adaptation, most of P700 and PC were in the reduced state. Once exposed to activated light, the two photosystems were activated successively and P700 began to oxidize. When the absorbance of P700 and PC^+ at

820 nm increases, the MR/MR_0 will show a downward trend (fast phase). Subsequently, as the electrons from PSII reach P700 and PC, the oxidation rate of P700 is slowed down, and the absorbance gradually decreases, which makes the reflection absorption curve of MR/MR_0 rise again, which is called the slow phase. $\Delta MR/MR_0$ was defined as the maximum reducible/oxidizable amplitude. The calculation equation is given according to Strasser *et al*. (2010) and Gao *et al*. (2014):

$$\Delta MR/MR_0 = (MR_0 - MR_{min})/MR_0$$

where MR_0 is the value at 0.7 ms and MR_{min} is the lowest point in 820-nm reflection curve.

$$V_{PSII} = V_{PSI} + V_{PSI+PSII}$$

where V_{PSI} indicates the maximum decrease in slope in the range of 0.7–3 ms of MR/MR_0:

$$V_{PSI} = (MR_{0.003s} - MR_{0.0007s})/[MR_0 \times (t_{0.003s} - t_{0.0007s})]$$

and $V_{PSI+VPSII}$ indicates the maximum increase in slope in the range of 7–300 ms of MR/MR_0:

$$V_{PSI+VPSII} = (MR_{0.3s} - MR_{0.007s})/[MR_0 \times (t_{0.3s} - t_{0.007s})]$$

Total Mn content and translation factor: The different organs (roots, stems, and leaves) of the harvested *L. lucidum* and *M. azedarach* were washed with pure water. The plant materials were kept at 105°C for killing out and then dried at 75°C for 48 h. The different organs were powdered and used to determine the Mn contents of different organs by ICP-AES (*Optima 8300*, *American Platinum Elmer*, USA) after digestion with HNO_3–$HClO_4$ (Han *et al*. 2016). Translation factor = Mn content in the leaves/Mn content in the roots.

Data analysis: Data were expressed as the mean value of each group consisting of three independent replicates. Results were presented as means ± standard error (SE). Statistical differences between measurements were analyzed using one-way analysis of variance (*ANOVA*), followed by the least significant difference (LSD) test by *SPSS 21*. *Pearson*'s correlation analysis was used to address the relationships between Mn contents and photosynthetic parameters in leaves on day 30 in *M. azedarach* and *L. lucidum*. All graphs were made by *Origin 9.1*. A $p<0.05$ was considered statistically significant.

Results

The contents of Mn in roots, stems, and leaves: The total Mn content in the Mn-treated *M. azedarach* and *L. lucidum* roots, stems, and leaves on day 30 was significantly increased compared to that of the control groups, and such elevation corresponded to the increasing Mn treatment. This increasing trend was observed under all treatment groups in all components of both tree species, except for the roots in the L1-treated group compared to that of the L2-treated group of *M. azedarach*. The Mn concentrations were the highest in the roots, followed by that of the leaves and stems (Fig. 1).

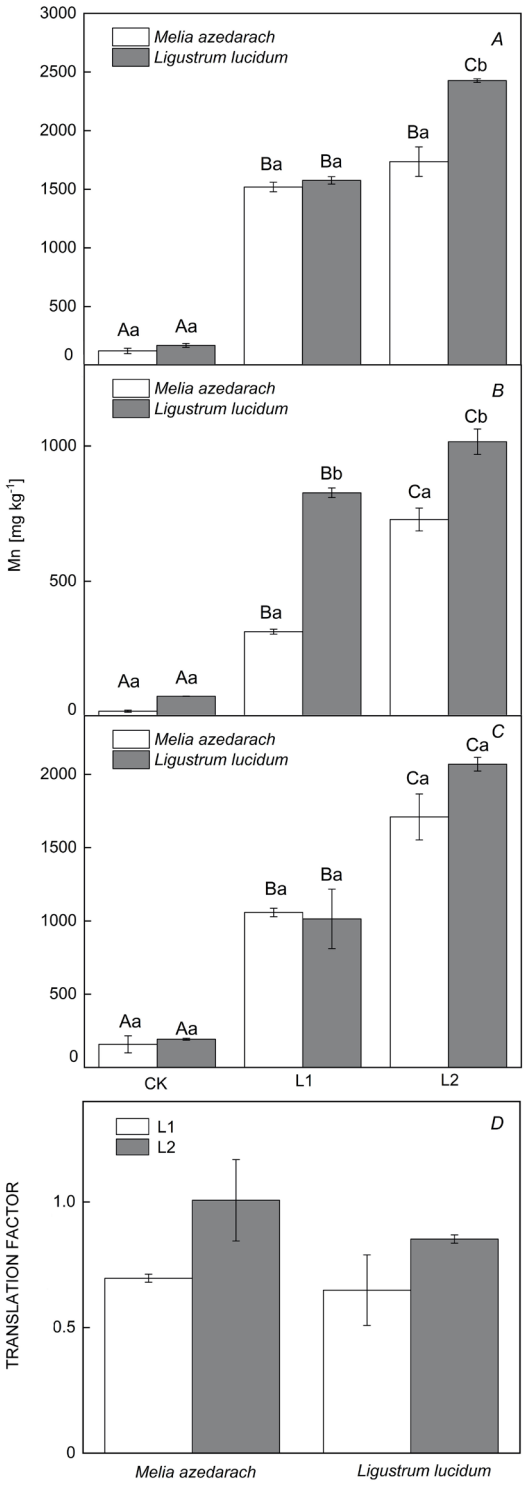

Fig. 1. The contents of Mn in roots (*A*), stems (*B*), and leaves (*C*) and the translocation factor (*D*) of *Melia azedarach* and *Ligustrum lucidum* in the Mn-treated groups on day 30. L1 – 0.5 mmol Mn treatment; L2 – 1 mmol Mn treatment. The data represent mean ± SE, $n = 5$. *Different capital letters* represent significant difference between different Mn treatments in the same organ of plant and the same tree species ($p<0.05$). *Different lowercase letters* represent significant difference between different tree species in the same organ of plant and the same Mn treatment ($p<0.05$)

The Mn content in the stems of *L. lucidum* under Mn treatments was significantly higher compared to *M. azedarach* in L1 and L2 treatment. There was no significant difference in the roots and leaves of *L. lucidum* and *M. azedarach* in all Mn-treated groups, except for that in the roots of the L2-treated group (Fig. 1).

The translation factors of both tree species increased with the increase of Mn concentration. The increased amplitude of the translation factor in *M. azedarach* was higher than that of *L. lucidum*.

Gas exchange: Mn stress decreased the P_N, g_s, and CE but increased the C_i for both tested tree species compared with controls (Table 1). For g_s and C_i, there was no significant difference between the Mn treatment groups and the control for both tested tree species (Table 1). P_N and CE significantly decreased in L2-treated groups compared with those of the control in both tree species, and there was no significant difference between the L1-treated groups and the control in both tree species (Table 1).

OJIP curve and light-induced modulated 820-nm reflection (MR/MR$_0$) kinetics: All OJIP transients from the leaves of the Mn-treated groups and the controls showed a typical polyphasic rise, and the basic process was OJIP. The values of F_0 showed a gradual increase in response to Mn treatment of *M. azedarach* and *L. lucidum* (Fig. 2*A*,*F*). The fluorescence induction curve of *M. azedarach* and *L. lucidum* did not show a considerable change in response to Mn excess on day 10. However, *M. azedarach* and *L. lucidum* exhibited a prominent rise of fluorescence intensity at L, K, J, and I points of the transient curve in response to Mn excess on day 30. In L2-treated groups on day 30, the increases of L, K, J, and I were higher in *M. azedarach* compared to *L. lucidum* (Fig. 2*B*,*C*,*G*,*H*). The maximum amplitude of the IP-phase progressively decreased with the increase of Mn concentration and the treatment time for both tested tree species. *M. azedarach* showed a faster decrease in the IP-phase compared to *L. lucidum* (Fig. 2*D*,*I*).

Under Mn stress, MR/MR$_0$ kinetics were changed in both tree species. As shown in Fig. 2, the rate of fast decline of the MR/MR$_0$ curve changed from 10 to 30 d of Mn stress. MR_{min} increased and the time to reach the MR_{min} shifted forward. V_{PSI} decreased but not significantly in response to Mn treatment of *L. lucidum* on 10 and 30 d (Table 2). The V_{PSI} of *M. azedarach* decreased but not significantly on day 10 but decreased significantly in the L1- and L2-treated groups compared with that of the controls (Table 2). For the slow rising phase of MR/MR$_0$, the $V_{PSI+PSII}$ decreased but not significantly in response to Mn treatment of *L. lucidum* on 10 and 30 d (Table 2). $V_{PSI+PSII}$ of *M. azedarach* decreased but not significantly on day 10 but decreased significantly in the L1- and L2-treated groups compared with that of the controls. V_{PSII} decreased but not significantly in response to Mn treatment of *L. lucidum* on 10 and 30 d. V_{PSII} of *M. azedarach* decreased but not significantly on day 10 but decreased significantly in the L1- and L2-treated groups compared with that of the controls (Fig. 2*E*,*J*; Table 2).

Quantum efficiency and FPs: On day 10, PI_{ABS}, F_V/F_M, S_m, Φ_{E0}, ψ_{E0}, and δ_{R0} decreased but not significantly in L1- and L2-treated groups compared with those of the controls (Fig. 3). M_0 and W_K increased but not significantly for both tree species in L1- and L2-treated groups compared with those of the controls (Fig. 3*B*,*D*). The W_K in *L. lucidum* in L2-treated groups significantly increased compared with that of the controls (Fig. 3*D*).

For *M. azedarach*, W_K in L2-treated groups and M_0 in L1 and L2 treatment groups significantly increased compared with those of the controls, while PI_{ABS}, F_V/F_M, and Φ_{E0} in L2 treatment groups significantly decreased compared with those of the controls on day 30 (Fig. 3). PI_{ABS} and F_V/F_M in L1 treatment groups significantly decreased compared with those of the controls on day 30 (Fig. 3*A*,*E*). S_m, δ_{R0}, and ψ_{E0} decreased but not significantly compared with those of the controls in L1 and L2 treatment groups on day 30 (Fig. 3*C*,*F*,*H*).

For *L. lucidum*, W_K and M_0 in L2 treatment groups significantly increased compared with those of the controls, while PI_{ABS}, F_V/F_M, and S_m in L2 treatment groups significantly decreased compared with those of the controls on day 30. Φ_{E0}, δ_{R0}, and ψ_{E0} decreased but not significantly compared with those of the controls in L1 and L2 treatment groups on day 30 (Fig. 3).

Effect of special energy fluxes or activities per reaction center: Mn stress increased but not significantly ABS/RC, TR$_0$/RC, and DI$_0$/RC on day 10 but decreased RE$_0$/RC in *M. azedarach*. The ABS/RC, TR$_0$/RC, and DI$_0$/RC increased significantly compared with those of the

Table 1. Changes in net photosynthetic rate (P_N), stomatal conductance (g_s), intercellular CO_2 concentration (C_i), and carboxylation efficiency (CE) in the control and Mn-treated groups on day 30 in *Melia azedarach* and *Ligustrum lucidum*. The data represent mean ± SE (n = 5) and values followed by *different capital letters* represent significant difference between Mn treatments in the same tree species (p<0.05). CK – control; L1 – 0.5 mmol Mn treatment; L2 – 1 mmol Mn treatment.

	Melia azedarach			*Ligustrum lucidum*		
	CK	L1	L2	CK	L1	L2
P_N [μmol m^{-2} s^{-1}]	5.61 ± 0.58^A	4.83 ± 0.23^{AB}	3.52 ± 0.44^B	5.46 ± 0.23^A	5.16 ± 0.41^{AB}	4.02 ± 0.48^B
g_s [mol m^{-2} s^{-1}]	0.057 ± 0.008^A	0.045 ± 0.004^A	0.035 ± 0.001^A	0.033 ± 0.001^A	0.033 ± 0.002^A	0.031 ± 0.007^A
C_i [μmol mol^{-1}]	213.94 ± 16.23^A	203.63 ± 7.93^A	211.00 ± 14.15^A	119.87 ± 2.76^A	121.27 ± 16.87^A	158.84 ± 18.28^A
CE [mol m^{-2} s^{-1}]	0.051 ± 0.005^A	0.030 ± 0.002^{AB}	0.023 ± 0.003^B	0.078 ± 0.002^A	0.050 ± 0.002^{AB}	0.033 ± 0.002^B

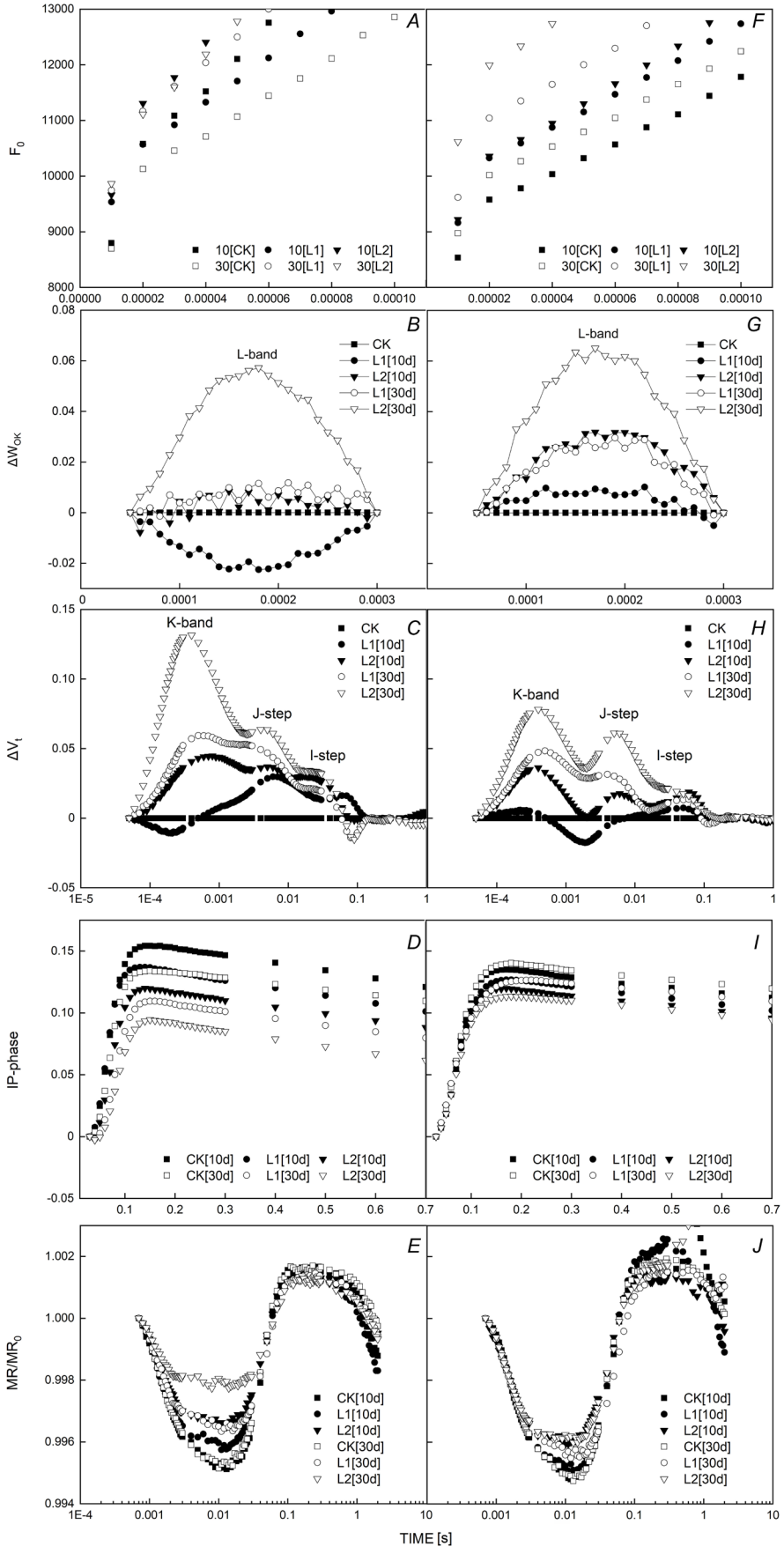

Fig. 2. Effects of excess Mn on the different expressions of relative variable fluorescence derived from the average OJIP transient and the kinetics of prompt fluorescence and modulated 820-nm reflection of *Melia azedarach* (*A–E*) and *Ligustrum lucidum* (*F–J*) on day 10 and day 30. CK – control; L1 – 0.5 mmol Mn treatment; L2 – 1 mmol Mn treatment. F_0 – minimal recorded fluorescence intensity; ΔW_{OK} – the difference between the CK groups and the treated groups in the relative fluorescence between O and K; ΔV_t – the difference between the CK groups and the treated groups in the relative fluorescence between O and P; IP-phase – the amplitude of the IP-phase; MR/MR_0 – the maximum reducible/oxidizable amplitude.

Table 2. The parameters of the kinetics of prompt fluorescence and modulated 820-nm reflection on day10 and 30 in *Melia azedarach* and *Ligustrum lucidum*. The data represent mean ± SE (n = 5) and values followed by *different capital letters* represent significant difference between different Mn treatments in the same tree species and stress time (p<0.05). V_{PSI} – maximum decrease in slope in the range of 0.7–3 ms of MR/MR_0; $V_{PSI+PSII}$ – maximum increase in slope in the range of 7–300 ms of MR/MR_0; V_{PSII} – the PSII activity.

	Melia azedarach			*Ligustrum lucidum*		
	CK	L1	L2	CK	L1	L2
Mn-stress for 10 days						
V_{PSI}	1.672 ± 0.211^A	1.511 ± 0.003^A	1.301 ± 0.213^A	1.676 ± 0.117^A	1.630 ± 0.001^A	1.475 ± 0.119^A
$V_{PSI+PSII}$	0.021 ± 0.035^A	0.019 ± 0.000^A	0.017 ± 0.035^A	0.022 ± 0.147^A	0.024 ± 0.003^A	0.018 ± 0.150^A
V_{PSII}	1.693 ± 0.052^A	1.530 ± 0.002^A	1.318 ± 0.054^A	1.698 ± 0.160^A	1.655 ± 0.001^A	1.493 ± 0.161^A
Mn-stress for 30 days						
V_{PSI}	1.618 ± 0.152^A	1.301 ± 0.001^B	0.806 ± 0.154^B	1.619 ± 0.042^A	1.458 ± 0.001^A	1.434 ± 0.043^A
$V_{PSI+PSII}$	0.021 ± 0.109^A	0.016 ± 0.001^B	0.011 ± 0.110^C	0.023 ± 0.085^A	0.019 ± 0.002^A	0.019 ± 0.087^A
V_{PSII}	1.639 ± 0.100^A	1.317 ± 0.001^B	0.817 ± 0.101^B	1.642 ± 0.199^A	1.477 ± 0.002^A	1.453 ± 0.200^A

controls, but the RE_0/RC increased in the L2 treatment group compared with the controls of *L. lucidum* on day 10 (Table 3).

Mn stress significantly increased TR_0/RC, ABS/RC, and DI_0/RC in the L2 treatment groups compared with those of the controls for *M. azedarach* and *L. lucidum* on day 30. RE_0/RC increased but not significantly in the L1 and L2 treatment groups compared with that of the controls for *L. lucidum* but decreased but not significantly in the L1 and L2 treatment groups of *M. azedarach* (Table 3).

Correlation analysis: In *L. lucidum*, *Pearson*'s correlation analysis showed that PI_{ABS} was significantly positively correlated to Φ_{E0} and CE. The Mn concentration in leaves was significantly negatively correlated to PI_{ABS}. The Mn concentration in leaves was significantly negatively correlated to Φ_{E0}. There were no significant relationships between CE and V_{PSI}, CE and V_{PSII} (Table 4).

In *M. azedarach*, *Pearson*'s correlation analysis showed that PI_{ABS} was significantly positively correlated to Φ_{E0} and CE. Φ_{E0} was significantly positively correlated to CE. V_{PSI} and V_{PSII} were significantly positively correlated to CE. The Mn concentration in leaves was significantly negatively correlated to PI_{ABS}, Φ_{E0}, V_{PSI}, and V_{PSII} (Table 4).

Discussion

Mn-induced decrease of the PSII activity: It is well known that the functions of PSII (donor and acceptor sides) and the electron-transfer chain might be damaged by the toxicity of heavy metals (Belatik *et al.* 2013, Li and Zhang 2015, Lin and Jin 2018). The Chl fluorescence transient (OJIP transient) can be used as a tool to assess photosynthesis (Kalaji and Loboda 2007). The O–J reflects the state of the reduction of the acceptor side of PSII. The Mn-induced K-step in the OKJIP at 300 μs was consistent with the results obtained from wheat under Mn stress (Fig. 2*C*,*H*) (Macfie and Taylor 1992). The increase in W_K might be related to an inactivation of the oxygen-evolving complex (OEC) (Strasser 1997, Stirbet *et al.* 2014, Chang *et al.* 2017), and the OEC splits water molecules to provide electrons to PSII reaction centers. Schmidt *et al.* (2016) found that the positive K-band can be observed in the seeds of two barley genotypes under Mn deficiency for a damaged and dysfunctional OEC. The same phenomenon was observed in our study. With the increase in Mn content and duration of stress, W_K gradually increased and reached the maximum in L2 groups on day 30. These results indicate the photodamage to the OEC that leads to a disturbance of electron transfer from the donor side to the acceptor side of PSII (Fig. 2). The K-band in *M. azedarach* was higher than that in *L. lucidum*, indicating that the OEC in *M. azedarach* is more vulnerable to Mn toxicity. The J-step represents the redox state of the first electron acceptor of PSII (Q_A) and the accumulation of Q_A (Mehta *et al.* 2010). The relative fluorescence intensity (ΔV_t) of the J-step was higher in Mn-treated groups in both trees compared with that of the controls, indicating that the electron transfer chain of PSII was inhibited, leading to the accumulation of Q_A^- (Jiang *et al.* 2008, Mlinarić *et al.* 2017). The J–I phase represents the change of the PQ pool (Fig. 2*C*,*H*). The relative fluorescence intensity (ΔV_t) of the I-step was higher in Mn-treated groups in both trees compared with that of the controls, indicating the accumulation of $Q_A^-Q_B^-$ (Gomes *et al.* 2012). In the present study, we found that electron transport downstream of Q_A was significantly reduced by Mn stress in both trees. This result is supported by the significant increase in M_0 and the significant decrease in S_m (Fig. 3*B*,*F*). When the electron transport downstream of Q_A was inhibited by DCMU (Strasser *et al.* 1995), the M_0 increased. S_m reflects the size of the PQ pool on the receptor side of the PSII reaction center and the energy required to completely reduce Q_A. The more electrons that enter the electron transfer chain from Q_A^-, the longer it takes to reach F_M, the greater the value of S_m. But in the present study, the S_m and F_M (Figs. 2*D*,*I*; 3*F*) decreased significantly in L2 groups on day 30, suggesting that Mn excess decreased the size of the PQ pool and inhibited the acceptor of PSII. These results were supported by the decreased value of ψ_{E0} and Φ_{E0} (Fig. 3*C*,*G*), leading to an inhibition in the acceptor side of PSII.

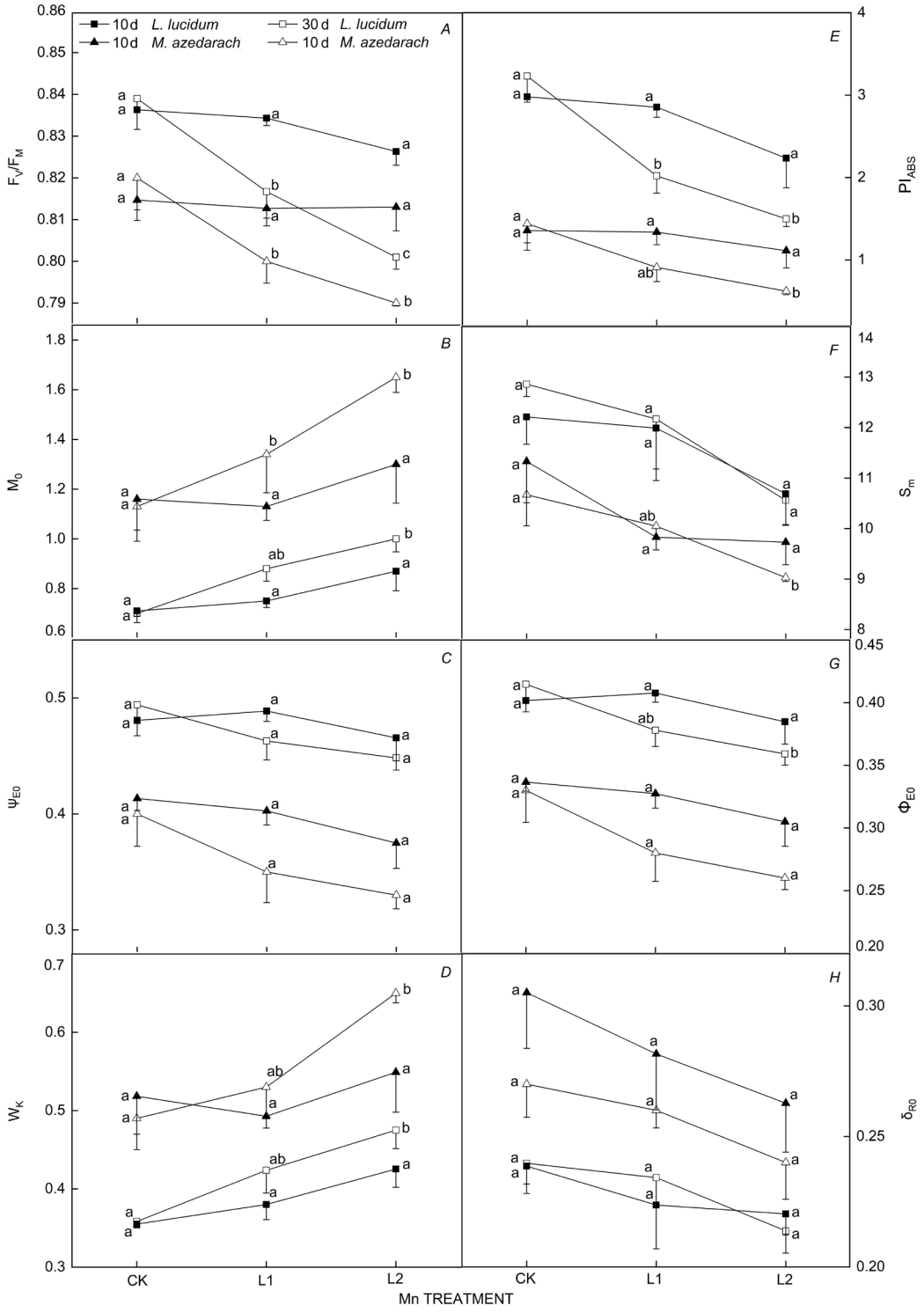

Fig. 3. Changes of yields or flux ratios (ψ_{E0}, δ_{R0}), PI_{ABS}, W_K, S_m, ψ_{E0}, $\Phi_{E0,}$ and F_V/F_M in the control and Mn-treated groups on day 10 and 30 in *Ligustrum lucidum* and *Melia azedarach*. CK – control; L1 – 0.5 mmol Mn treatment; L2 – 1 mmol Mn treatment. The data represent mean ± SE (n = 5) and values followed by *different lowercase letters* represent significant difference between different Mn treatments in the same tree species and stress time (p<0.05). F_V/F_M – maximum quantum use efficiency; M_0 – approximated initial slope of the fluorescence transient; ψ_{E0} – probability that a trapped exciton moves an electron into the electron transport chain beyond Q_A; W_K – relative variable fluorescence at the K-step to the amplitude $F_J - F_0$; PI_{ABS} – performance index; S_m – normalized total complementary area above the OJIP transient (reflecting single-turnover Q_A reduction events);Φ_{E0} – quantum yield for electron transport; δ_{R0} – efficiency with which an electron can move from the reduced intersystem electron acceptors to the PSI end electron acceptors.

Table 3. Mn effect on the special energy fluxes or activities per reaction center on day10 and 30 in *Melia azedarach* and *Ligustrum lucidum*. The data represent mean ± SE (n = 5) and values followed by *different capital letters* represent significant difference between different Mn treatments in the same tree species and stress time (p<0.05). ABS/RC – absorption flux (of antenna Chls) per RC (also a measure of PSII apparent antenna size); TR_0/RC – trapped energy flux (leading to Q_A reduction) per RC at t = 0; RE_0/RC – the flux of electrons transferred from Q_A^- to final PSI acceptors per PSII at t = 0; DI_0/RC – dissipated energy flux per RC at t = 0.

	Melia azedarach			*Ligustrum lucidum*		
	CK	L1	L2	CK	L1	L2
Mn-stress for 10 days						
ABS/RC	2.32 ± 0.19^{A}	2.22 ± 0.07^{A}	2.46 ± 0.23^{A}	1.58 ± 0.00^{A}	1.69 ± 0.08^{AB}	1.91 ± 0.11^{B}
TR_0/RC	1.89 ± 0.16^{A}	1.81 ± 0.05^{A}	1.99 ± 0.17^{A}	1.32 ± 0.01^{A}	1.41 ± 0.07^{AB}	1.58 ± 0.08^{B}
RE_0/RC	0.24 ± 0.03^{A}	0.20 ± 0.02^{A}	0.20 ± 0.02^{A}	0.15 ± 0.01^{A}	0.15 ± 0.01^{A}	0.16 ± 0.01^{A}
DI_0/RC	0.43 ± 0.03^{A}	0.42 ± 0.02^{A}	0.46 ± 0.06^{A}	0.26 ± 0.01^{A}	0.28 ± 0.02^{AB}	0.33 ± 0.02^{B}
Mn-stress for 30 days						
ABS/RC	2.21 ± 0.19^{A}	2.44 ± 0.19^{AB}	2.96 ± 0.05^{B}	1.59 ± 0.04^{A}	1.93 ± 0.15^{AB}	2.19 ± 0.09^{B}
TR_0/RC	1.80 ± 0.14^{A}	1.94 ± 0.13^{AB}	2.33 ± 0.04^{B}	1.34 ± 0.03^{A}	1.58 ± 0.11^{AB}	1.76 ± 0.08^{B}
RE_0/RC	0.20 ± 0.01^{A}	0.18 ± 0.00^{A}	0.18 ± 0.01^{A}	0.16 ± 0.01^{A}	0.17 ± 0.02^{A}	0.17 ± 0.01^{A}
DI_0/RC	0.41 ± 0.05^{A}	0.50 ± 0.05^{AB}	0.63 ± 0.01^{B}	0.26 ± 0.01^{A}	0.36 ± 0.04^{B}	0.44 ± 0.01^{B}

Table 4. *Pearson*'s correlation coefficients between Mn concentration, CO_2 fixation, and photosynthesis parameters in leaves on day 30 in *Melia azedarach* and *Ligustrum lucidum*. *Correlation is significant at the 0.05 level (p<0.05). **Correlation is significant at the 0.01 level (p<0.01). CE – carboxylation efficiency; PI_{ABS} – performance index; V_{PSI} – maximum decrease in slope in the range of 0.7–3 ms of MR/MR_0; V_{PSII} – the activity of PSII; Φ_{E0} – quantum yield for electron transport; Mn – the Mn concentration in leaves.

	Melia azedarach				*Ligustrum lucidum*			
	PI_{ABS}	Φ_{E0}	V_{PSI}	V_{PSII}	PI_{ABS}	Φ_{E0}	V_{PSI}	V_{PSII}
CE	0.877^{**}	0.779^{*}	0.891^{**}	0.891^{**}	0.717^{*}	0.447	0.525	0.529
Mn	-0.771^{*}	-0.731^{*}	-0.852^{**}	-0.853^{**}	-0.837^{**}	-0.802^{**}	–0.318	–0.321
Φ_{E0}	0.964^{**}	1	0.623	0.623	0.910^{**}	1	0.509	0.512

The JIP-test can be used as a tool to detect and quantify the changes in photosynthetic apparatus under heavy metal stress (Kalaji and Loboda 2007, Leplat *et al*. 2016). The increased F_0 and the decreased F_M can be observed in this study for both trees in L1 and L2 treatment on day 10 and day 30 (Fig. 2*A*,*D*,*F*,*I*). This phenomenon is most apparent in L2 treatment groups on day 30. According to previous studies (Yamane *et al*. 1997, Kalaji *et al*. 2017), these results may suggest that the increased F_0 and decreased F_M might be related to the inactivation of the PSII reaction center and the destabilization of PSII. The significant increase in both ABS/RC and TR_0/RC (Table 3) might indicate inactivation of a certain part of PSII RCs, which was most likely due to inactivation of the OEC as well as the transformation of active RCs to silent ones (Strasser *et al*. 2004, Zhang *et al*. 2017). Additionally, the significant increase in ABS/RC and the positive L-band reflect the loss of connectivity and PSII RCs become more vulnerable to damage (Li *et al*. 2010). As a result, the DI_0/RC increased significantly in L2 treatment on day 30 in both tested trees. Combined with the changes in the above parameters, Mn caused a decrease in overall PSII activity supported by the significant decrease in PI_{ABS} (Fig. 3*B*).

Mn-excess affected the oxidation and reduction of PSI: The IP-phase is associated with the number of reduced end acceptors at the PSI acceptor side, and the reduced δ_{R0} represents the electron flow to the PSI acceptor side if inhibited (Li *et al*. 2010, Desotgiu *et al*. 2012). The reduction in amplitude of the IP-phase (Fig. 2*D*,*I*) and δ_{R0} (Fig. 3*H*) may be caused by the inactivation of the PSI acceptor side or the inhibition in electron transport from the donor side of PSII to the acceptor side of PSI. In this study, with an increase of Mn concentration and stress duration, it can be observed that the 820-nm absorption value of the fast phase gradually decreased, indicating that the rate of independent oxidation and reduction of P700 slowed down before electron transport from PSII to P700 (Gao *et al*. 2014). This phenomenon was supported by the significant decrease in V_{PSI} in *M. azedarach* in the L2 treatment group on day 30, indicating that the photochemical activity of PSI decreased. Furthermore, the reoxidation rate of PQH_2 after illumination was affected by Mn stress (Table 2). Similarly, the $V_{PSI+PSII}$ also decreased significantly in *M. azedarach* in the L1 and L2 treatment groups on day 30, which means that the rate of electron reoxidation and reduction of P700 and PC from PSII slowed down, and the coordination of electron transport between the PSI and PSII decreased. V_{PSII} represents the rate of electron transfer from PSII to P700 (Fig. 2*E*,*J*). The significant decrease of V_{PSII} in *M. azedarach* in the L2 treatment group on day 30 reflected that the electron transfer from PQH_2 to PSI was blocked

due to the disordering of electron transport downstream of Q_A (Fig. 2*E*,*J*; Table 2). Mn stress decreased the PSII activity, inhibited the re-reduction of P700, and affected the ability of electron transfer on the acceptor side of PSII (included the PSI), suggesting that the connectivity between PSI and PSII was damaged under Mn excess in *M. azedarach* in the L1 and L2 treatment groups on day 30 (Fig. 2*E*,*J*). But in *L. lucidum*, the parameters (V_{PSI}, $V_{PSI+PSII}$, V_{PSII}) decreased but not significantly; this may be because PSI still maintains activity under Mn stress (Fig. 2*E*,*J*; Table 2) (Gao *et al*. 2014, Chu *et al*. 2018).

Mn excess affected the leaf CO_2 assimilation: Great decreases in net photosynthetic rate (P_N) and leaf CO_2 assimilation (CE) in the L2 groups revealed the vulnerability of photosynthesis in *M. azedarach* and *L. lucidum* to Mn treatment (Table 1). In a previous investigation, Li *et al*. (2010) have shown that the decrease in CE in response to excess Mn is caused by impaired electron transport capacity rather than stomatal factors. In the current study, since the decrease in stomatal conductance (g_s) was accompanied by an increase in intercellular CO_2 concentration (C_i) (Table 1), Mn excess caused nonstomatal factors to impact photosynthesis in *M. azedarach* and *L. lucidum* (Xie *et al*. 2018).

Jiang *et al*. (2008) have found that the decreased CE in response to aluminum (Al) stress for the impaired electron transport chain is accompanied by the limitation in the reduction of the PSI end electron acceptors through the positive relationship between CE and the IP-phase. In *L. lucidum*, the decrease of CE was significantly and negatively related to the increase of the Mn concentration, but significantly and positively related to the decrease of PI_{ABS} on day 30 (Table 4). There was no significant relationship between the CE and V_{PSI} or the Mn concentration and V_{PSI}. These results suggest that excess Mn impaired the activity of PSII but the PSI of *L. lucidum* was stable under the Mn excess. The decrease in CE might be related to the damage of PSII and the electron transport chain from the donor side of PSII to Q_A. However, different results were shown in *M. azedarach*. In *M. azedarach*, the Mn concentrations in leaves were significantly and negatively related to PI_{ABS}, V_{PSI}, V_{PSII}, and Φ_{E0}, while CE was significantly and positively related to PI_{ABS}, V_{PSI}, V_{PSII}, and Φ_{E0} (Table 4). These results suggest that the excess Mn damaged the activity of PSII and changed the state of oxidation and reduction of PSI. As a result, it further affected the electron transfer chain and its stability between PSII and PSI. The decreased CE might be related to the damaged electron transfer chain and the inactive PSII and the state of oxidation and reduction of PSI.

Notably, reduction of P_N and CE was more significant under Mn excess in the L2 treatment group in *M. azedarach* than in *L. lucidum* (Table 1). This phenomenon may be caused by the fact that when compared to *M. azedarach*, *L. lucidum* still maintained relatively stable photosynthetic capacity and showed better tolerance under the Mn excess. Another possible reason is that the translation factor of *M. azedarach* was higher than that of *L. lucidum*, indicating that more Mn^{2+} was transported from the roots to the leaves in *M. azedarach.* This result was consistent with the findings of Bernardini *et al.* (2016) that zinc is transported to the leaves of plants, leading to the decrease of CE, while lead (Pb) was accumulated mainly in the roots, which has a slight effect on gas-exchange parameters.

Conclusions: In this study, we concluded that excess Mn harmed photosynthesis in *L. lucidum* and *M. azedarach*. The reduction in leaf CO_2 assimilation and the net photosynthetic rates in both tested trees were mainly caused by the damage of the photosynthetic electron transport chain from the donor side of PSII to the reduction of end acceptors of PSI. The change of the specific energy fluxes (per active PSII) suggested that the reaction center of PSII was inactivated under Mn excess in both tested trees. Mn excess decreased the activity of PSII owing to the inactive OEC and the limitation in electron transport downstream of Q_A^- in both tested trees. The state of the oxidation and reduction in PSI under Mn was different in both tested tree species. The rate of photochemical activity of PSI decreased (only in *M. azedarach*) for the independent oxidation while reduction of P700 was slowed down. Comparatively, Mn stress exerted less inhibitory effects on photosynthesis in *L. lucidum*. Therefore, the photosynthetic performance showed more tolerance in *L. lucidum* compared to *M. azedarach* under Mn stress.

References

Aranjuelo I., Doustaly F., Cela J. *et al*.: Glutathione and transpiration as key factors conditioning oxidative stress in *Arabidopsis thaliana* exposed to uranium. – Planta **239**: 817-830, 2014.

Barón M., Arellano J.B., Gorgé J.L.: Copper and photosystem II: A controversial relationship. – Physiol. Plantarum **94**: 174-180, 1995.

Belatik A., Hotchandani S., Tajmir-Riahi H.A., Carpentier R.: Alteration of the structure and function of photosystem I by Pb^{2+}. – J. Photoch. Photobio. B **123**: 41-47, 2013.

Bernardini A., Salvatori E., Guerrini V. *et al*.: Effects of high Zn and Pb concentrations on *Phragmites australis* (Cav.) Trin. Ex. Steudel: Photosynthetic performance and metal accumulation capacity under controlled conditions. – Int. J. Phytoremediat. **18**: 16-24, 2016.

Ceppi M.G., Oukarroum A., Çiçek N. *et al*.: The IP amplitude of the fluorescence rise OJIP is sensitive to changes in the photosystem I content of leaves: a study on plants exposed to magnesium and sulfate deficiencies, drought stress and salt stress. – Physiol. Plantarum **144**: 277-288, 2012.

Chang W., Chen C., Dong H., Zhang C.: Artificial Mn4-oxido complexes mimic the oxygen-evolving center in photosynthesis. – Sci. Bull. **62**: 665-668, 2017.

Che X.K., Ding R.R., Li Y.T. *et al*.: Mechanism of long-term toxicity of CuO NPs to microalgae. – Nanotoxicology **12**: 923-939, 2018.

Chu J.J., Zhu F., Chen X.Y. *et al*.: Effects of cadmium on photosynthesis of *Schima superba* young plant detected by chlorophyll fluorescence. – Environ. Sci. Pollut. R. **25**: 10679-10687, 2018.

Demmig-Adams B., Stewart J.J., Adams III W.W.: Environmental regulation of intrinsic photosynthetic capacity: an integrated view. – Curr. Opin. Plant Biol. **37**: 34-41, 2017.

Desotgiu R., Pollastrini M., Cascio C. *et al*.: Chlorophyll *a*

fluorescence analysis along a vertical gradient of the crown in a poplar (Oxford clone) subjected to ozone and water stress. – Tree Physiol. **32**: 976-986, 2012.

Dewez D., Geoffroy L., Vernet G., Popovic R.: Determination of photosynthetic and enzymatic biomarkers sensitivity used to evaluate toxic effects of copper and fludioxonil in alga *Scenedesmus obliquus*. – Aquat. Toxicol. **74**: 150-159, 2005.

Farmer E.E., Mueller M.J.: ROS-mediated lipid peroxidation and RES-activated signaling. – Annu. Rev. Plant Biol. **64**: 429-450, 2013.

Flexas J., Medrano H.: Drought-inhibition of photosynthesis in C_3 plants: Stomatal and non-stomatal limitations revisited. – Ann. Bot.-London **89**: 183-189, 2002.

Fodor F.: Physiological responses of vascular plants to heavy metals. – In: Prasad M.N.V., Strzałka K. (ed.): Physiology and Biochemistry of Metal Toxicity and Tolerance in Plants. Pp. 149-177. Springer, Dordrecht 2002.

Gao J., Li P.M., Ma F.W., Goltsev V.: Photosynthetic performance during leaf expansion in *Malus micromalus* probed by chlorophyll *a* fluorescence and modulated 820 nm reflection. – J. Photoch. Photobio. B **137**: 144-150, 2014.

Gomes M.T.G., da Luz A.C., dos Santos M.R. *et al.*: Drought tolerance of passion fruit plants assessed by the OJIP chlorophyll *a* fluorescence transient. – Sci. Hortic.-Amsterdam **142**: 49-56, 2012.

González E., Lynch J.: Effects of manganese toxicity on leaf CO_2 assimilation of contrasting common bean genotypes. – Physiol. Plantarum **101**: 872-880, 2006.

Gururani M.A., Upadhyaya C.P., Strasser R.J. *et al.*: Evaluation of abiotic stress tolerance in transgenic potato plants with reduced expression of PSII manganese stabilizing protein. – Plant. Sci. **198**: 7-16, 2013.

Han Y.L., Zhang L.L., Yang Y.H. *et al.*: Pb uptake and toxicity to *Iris halophila* tested on Pb mine tailing materials. – Environ. Pollut. **214**: 510-516, 2016.

He B., Yun Z.J., Shi J.B., Jiang G.B.: Research progress of heavy metal pollution in China: Sources, analytical methods, status, and toxicity. – Chinese Sci. Bull. **58**: 134-140, 2012.

Huang W., Zhang S.B., Liu T.: Moderate photoinhibition of photosystem II significantly affects linear electron flow in the shade-demanding plant *Panax notoginseng*. – Front. Plant Sci. **9**: 637, 2018.

Jiang H.X., Chen L.S., Zheng J.G. *et al.*: Aluminum-induced effects on Photosystem II photochemistry in *Citrus* leaves assessed by the chlorophyll *a* fluorescence transient. – Tree Physiol. **28**: 1863-1871, 2008.

Kalaji H.M., Loboda T.: Photosystem II of barley seedlings under cadmium and lead stress. – Plant Soil Environ. **53**: 511-516, 2007.

Kalaji H.M., Schansker G., Brestič M. *et al.*: Frequently asked questions about chlorophyll fluorescence, the sequel. – Photosynth. Res. **132**: 13-66, 2017.

Khattak M.I., Jabeen R.: Detection of heavy metals in leaves of *Melia azedarach* and *Eucalyptus citriodora* as biomonitoring tools in the region of Quetta valley. – Pak. J. Bot. **44**: 675-681, 2012.

Kitao M., Lei T.T., Koike T.: Effects of manganese toxicity on photosynthesis of white birch (*Betula platyphylla* var. *japonica*) seedlings. – Physiol. Plantarum **101**: 249-256, 1997.

Kono M., Noguchi K., Terashima I.: Roles of the cyclic electron flow around PSI (CEF-PSI) and O_2-dependent alternative pathways in regulation of the photosynthetic electron flow in short-term fluctuating light in *Arabidopsis thaliana*. – Plant Cell Physiol. **55**: 990-1004, 2014.

Leplat F., Pedas P.R., Rasmussen S.K., Husted S.: Identification of manganese efficiency candidate genes in winter barley (*Hordeum vulgare*) using genome wide association mapping. – BMC Genomics **17**: 775, 2016.

Li Q., Chen L.S., Jiang H.X. *et al.*: Effects of manganese-excess on CO_2 assimilation, ribulose-1,5-bisphosphate carboxylase/oxygenase, carbohydrates and photosynthetic electron transport of leaves, and antioxidant systems of leaves and roots in *Citrus grandis* seedlings. – BMC Plant Biol. **10**: 42, 2010.

Li X., Zhang L.: Endophytic infection alleviates Pb^{2+} stress effects on photosystem II functioning of *Oryza sativa* leaves. – J. Hazard. Mater. **295**: 79-85, 2015.

Liang H.Z., Zhu F., Wang R.J. *et al.*: Photosystem II of *Ligustrum lucidum* in response to different levels of manganese exposure. – Sci. Rep.-UK **9**: 12568, 2019.

Lin M.Z., Jin M.F.: Soil Cu contamination destroys the photosynthetic systems and hampers the growth of green vegetables. – Photosynthetica **56**: 1336-1345, 2018.

Macfie S.M., Taylor G.J.: The effects of excess manganese on photosynthetic rate and concentration of chlorophyll in *Triticum aestivum* grown in solution culture. – Physiol. Plantarum **85**: 467-475, 1992.

Mehta P., Jajoo A., Mathur S., Bharti S.: Chlorophyll *a* fluorescence study revealing effects of high salt stress on Photosystem II in wheat leaves. – Plant Physiol. Bioch. **48**: 16-20, 2010.

Millaleo R., Reyes-Díaz M., Alberdi M. *et al.*: Excess manganese differentially inhibits photosystem I versus II in *Arabidopsis thaliana*. – J. Exp. Bot. **64**: 343-354, 2013.

Miyata K., Ikeda H., Nakaji M. *et al.*: Rate constants of PSII photoinhibition and its repair, and PSII fluorescence parameters in field plants in relation to their growth light environments. – Plant Cell Physiol. **56**: 1841-1854, 2015.

Mlinarić S., Antunović Dunić J., Skendrović Babojelić M. *et al.*: Differential accumulation of photosynthetic proteins regulates diurnal photochemical adjustments of PSII in common fig (*Ficus carica* L.) leaves. – J. Plant Physiol. **209**: 1-10, 2017.

Moradi L., Ehsanzadeh P.: Effects of Cd on photosynthesis and growth of safflower (*Carthamus tinctorius* L.) genotypes. – Photosynthetica **53**: 506-518, 2015.

Nagajyoti P.C., Lee K.D., Sreekanth T.V.M.: Heavy metals, occurrence and toxicity for plants: a review. – Environ. Chem. Lett. **8**: 199-216, 2010.

Pätsikkä E., Aro E.-M., Tyystjärvi E.: Increase in the quantum yield of photoinhibition contributes to copper toxicity *in vivo*. – Plant Physiol. **117**: 619-627, 1998.

Qiao X.Q., Shi G.X., Jia R. *et al.*: Physiological and biochemical responses induced by lead stress in *Spirodela polyrhiza*. – Plant Growth. Regul. **67**: 217-225, 2012.

Rijstenbil J.W., Derksen J.W.M., Gerringa L.J.A. *et al.*: Oxidative stress induced by copper: defense and damage in the marine planktonic diatom *Ditylum brightwellii*, grown in continuous cultures with high and low zinc levels. – Mar. Biol. **119**: 583-590, 1994.

Schmidt S.B., Powikrowska M., Krogholm K.S. *et al.*: Photosystem II functionality in barley responds dynamically to changes in leaf manganese status. – Front. Plant Sci. **7**: 1772, 2016.

Sigfridsson K.G.V., Bernát G., Mamedov F., Styring S.: Molecular interference of Cd^{2+} with photosystem II. – BBA-Bioenergetics **1659**: 19-31, 2004.

Stirbet A., Lazár D., Kromdijk J., Govindjee: Chlorophyll *a* fluorescence induction: Can just a one-second measurement be used to quantify abiotic stress responses? – Photosynthetica **56**: 86-104, 2018.

Stirbet A., Riznichenko G.Yu., Rubin A.B., Govindjee: Modeling chlorophyll *a* fluorescence transient: Relation to

photosynthesis. – Biochemistry-Moscow+ **79**: 291-323, 2014.
Strasser B.J.: Donor side capacity of Photosystem II probed by chlorophyll *a* fluorescence transient. – Photosynth. Res. **52**: 147-155, 1997.
Strasser R.J., Srivastava A., Govindjee: Polyphasic chlorophyll *a* fluorescence transient in plants and cyanobacteria. – Photochem. Photobiol. **61**: 32-42, 1995.
Strasser R.J., Tsimilli-Michael M., Qiang S., Goltsev V.: Simultaneous *in vivo* recording of prompt and delayed fluorescence and 820-nm reflection changes during drying and after rehydration of the resurrection plant *Haberlea rhodopensis*. – BBA-Bioenergetics **1797**: 1313-1326, 2010.
Strasser R.J., Tsimilli-Michael M., Srivastava A.: Analysis of the chlorophyll *a* fluorescence transient. – In: Papageorgiou G.C., Govindjee (ed.): Chlorophyll *a* Fluorescence: A Signature of Photosynthesis. Advances in Photosynthesis and Respiration. Pp. 321-362. Springer, Dordrecht 2004.
Su M.J., Cai S.Z., Deng H.M. *et al*.: [Effects of cadmium and acid rain on cell membrane permeability and osmotic adjustment substance content of *Melia azedarach* L. seedlings.] – Acta Sci. Circum. **37**: 4436-4443, 2017. [In Chinese] doi: 10.13671/j.hjkxxb.2017.0216.
Suorsa M., Järvi S., Grieco M. *et al*.: PROTON GRADIENT REGULATION5 is essential for proper acclimation of *Arabidopsis* photosystem I to naturally and artificially fluctuating light conditions. – Plant Cell **24**: 2934-2948, 2012.
Suresh R., Foy C.D., Weidner J.R.: Effects of excess soil manganese on stomatal function in two soybean cultivars. – J. Plant Nutr. **10**: 749-760, 1987.
Tikkanen M., Mekala N.R., Aro E.-M.: Photosystem II photoinhibition-repair cycle protects Photosystem I from irreversible damage. – BBA-Bioenergetics **1837**: 210-215, 2014.
Tong F.P., Long Y.Z., Yi J.X. *et al*.: Characteristics of heavy metal accumulation in *Broussonetia papyrifera* in an antimony mine. – J. Food Agric. Environ. **9**: 701-705, 2011.
Trikshiqi R., Rexha M.: Heavy metal monitoring by *Ligustrum lucidum*, Fam: *Oleaceae* vascular plant as bio-indicator in Durres city. – Int. J. Curr. Res. **7**: 14415-14422, 2015.
Valladares F., Pearcy R.W.: Drought can be more critical in the shade than in the sun: a field study of carbon gain and photo-inhibition in a Californian shrub during a dry El Niño year. – Plant Cell Environ. **25**: 749-759, 2002.
Xie D.F., Zhang G.C., Xia X.X. *et al*.: The effects of phenolic acids on the photosynthetic characteristics and growth of *Populus* × *euramericana* cv. 'Neva' seedlings. – Photosynthetica **56**: 981-988, 2018.
Xue S., Zhu F., Wu C. *et al*.: Effects of manganese on the microstructures of *Chenopodium ambrosioides* L., a manganese tolerant plant. – Int. J. Phytoremediat. **18**: 710-719, 2015.
Yamane Y., Kashino Y., Koike H., Satoh K.: Increases in the fluorescence F_O level and reversible inhibition of Photosystem II reaction center by high-temperature treatments in higher plants. – Photosynth. Res. **52**: 57-64, 1997.
Yang Y.J., Liu T., Zhang S.B., Huang W.: Photoinhibition of oxygen-evolving complex and photosystem II at chilling stress in the tropical tree species *Dalbergia odorifera*. – Photosynthetica **58**: 245-252, 2020.
Yruela I., Pueyo J.J., Alonso P.J., Picorel R.: Photoinhibition of photosystem II from higher plants: Effect of copper inhibition. – J. Biol. Chem. **271**: 27408-27415, 1996.
Zhang L.T., Su F., Zhang C.H. *et al*.: Changes of photosynthetic behaviors and photoprotection during cell transformation and astaxanthin accumulation in *Haematococcus pluvialis* grown outdoors in tubular photobioreactors. – Int. J. Mol. Sci. **18**: 33, 2017.
Zhang Z.S., Jin L.Q., Li Y.T. *et al*.: Ultraviolet-B radiation (UV-B) relieves chilling-light-induced PSI photoinhibition and accelerates the recovery of CO_2 assimilation in cucumber (*Cucumis sativus* L.) leaves. – Sci. Rep.-UK **6**: 34455, 2016.